Asymmetric Hydrogenation

DOI: 10.1002/anie.201208774

Cooperative Catalysis through Noncovalent Interactions**

Weijun Tang, Steven Johnston, Jonathan A. Iggo, Neil G. Berry, Marie Phelan, Luyun Lian, John Bacsa, and Jianliang Xiao**

Noncovalent interactions, such as hydrogen bonding, electrostatic, π–π, CH–π, and hydrophobic forces, play an essential role in the action of nature's catalysts, enzymes. In the last decade these interactions have been successfully exploited in organocatalysis with small organic molecules.[1] In contrast, such interactions have rarely been studied in the well-established area of organometallic catalysis,[2] where electronic interactions through covalent bonding and steric effects imposed by bound ligands dictate the activity and selectivity of a metal catalyst. An interesting question is: What happens when an organocatalyst meets an organometallic catalyst? This unification has already created an exciting new space for both fields: cooperative catalysis, where reactants are activated simultaneously by both types of catalyst, thereby enabling reactivity and selectivity patterns inaccessible within each field alone.[3] However, the mechanisms by which the two catalysts cooperatively effect the catalysis remain to be delineated. We recently found that combining an achiral iridium catalyst with a chiral phosphoric acid allows for highly enantioselective hydrogenation of imines (Scheme 1).[4] To gain insight into the mechanism of this metal–organo cooperative catalysis, we studied the catalytic system with a range of techniques, including high pressure 2D-NMR spectroscopy, diffusion measurements, and NOE-constrained computation. Herein we report our findings.

To evaluate the mechanism, a simplified achiral complex **C** was used, which leads to [**C**$^+$][**A**$^-$] upon mixing, in situ or ex situ, with the chiral phosphoric acid **HA** through protonation at the amido nitrogen (Scheme 1). In the asymmetric hydrogenation of the model ketimine **1a**, [**C**$^+$][**A**$^-$] afforded 95% *ee* and full conversion. On the basis of related studies,[5] the hydrogenation can be broadly explained by the catalytic cycle shown in Scheme 1, that is, [**C**$^+$][**A**$^-$] activates H_2 to give the hydride **D** and protonated **1a**, which forms an ion pair with the phosphate affording [**1a**$^+$][**A**$^-$];[6,7] hydride transfer furnishes the amine product **2a** while regenerating [**C**$^+$][**A**$^-$]. Questions pertinent to possible iridium–phosphate cooperation then arise: 1) How does the chiral phosphoric acid induce asymmetry in the hydrogenation? and 2) Does the enantioselectivity result from **D** being formed enantioselectively from [**C**$^+$][**A**$^-$], from the phosphate salt [**1a**$^+$][**A**$^-$], or from interactions involving all three components?

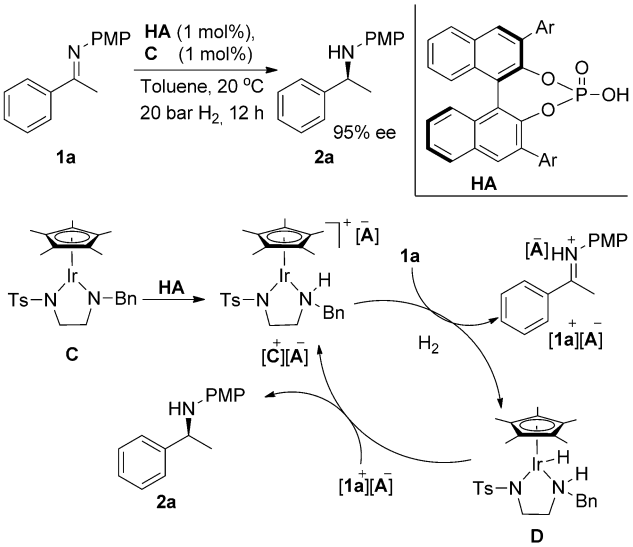

Scheme 1. Hydrogenation of imine with achiral **C** and chiral acid **HA** (PMP = *p*-methoxyphenyl, Ar = 2,4,6-triisopropylphenyl, Ts = tosyl, Bn = benzyl).

We looked first at how the formation of hydride **D** and its transfer into the substrate are influenced by the chiral acid **HA**. The studies were carried out in CH_2Cl_2 or CD_2Cl_2 owing to the low solubility of the various metal complexes in toluene. The catalytic hydrogenation is feasible in both solvents, giving a 95% *ee* in toluene and 85% *ee* in CH_2Cl_2 in the case of hydrogenation of **1a** with **C** and **HA** under the conditions given in Scheme 1. The solution NMR studies show that the ionic complex [**C**$^+$][**A**$^-$] is formed instantly on protonation of **C** (0.05 mmol) with one equivalent **HA** in CD_2Cl_2 (0.5 mL). Under H_2 pressure (> 1 bar), proton transfer from a [**C**$^+$]–H_2 dihydrogen intermediate (not observed) to **1a** converts [**C**$^+$] into the hydride **D** and affords the salt [**1a**$^+$][**A**$^-$].[7] Formation of **D** took place instantly even at −78 °C, and it is observed during catalytic turnover, thus indicating that the hydrogenation is rate-limited by the hydride transfer step.

[*] Dr. W. Tang,[+] S. Johnston,[+] Dr. J. A. Iggo, Dr. N. G. Berry, Dr. J. Bacsa, Prof. J. Xiao
Liverpool centre for Materials & Catalysis
Department of Chemistry, University of Liverpool
Liverpool L69 7ZD (UK)
E-mail: jxiao@liv.ac.uk
Homepage: http://pcwww.liv.ac.uk/~xiao
Dr. M. Phelan, Prof. L. Lian
NMR Centre for Structural Biology, Institute of Integrative Biology
University of Liverpool
Liverpool, L69 7ZB (UK)
[+] These authors contributed equally to this work.

[**] We thank EPRSC for funding support to W.J.T. and S.J. on grant EP/G031444, the University of Liverpool for support of the NMR Centre for Structural Biology, and the EPSRC National Mass Spectrometry Service Centre for mass analysis.
Supporting information for this article is available on the WWW under http://dx.doi.org/10.1002/anie.201208774.

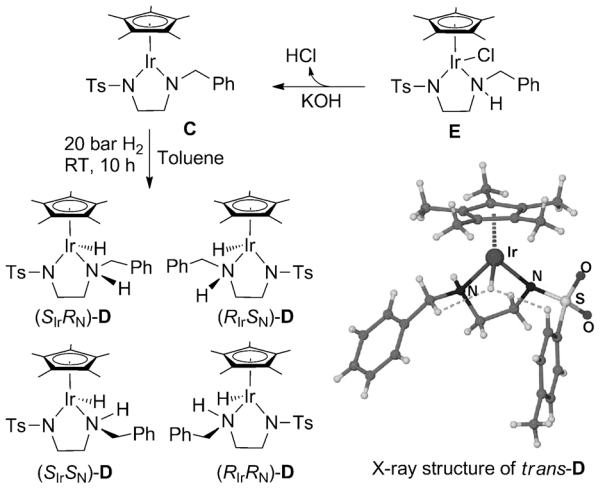

Scheme 2. Formation of racemic hydrides **D** by hydrogenating **C** generated from **E** and the X-ray structure of *trans*-**D**.[17]

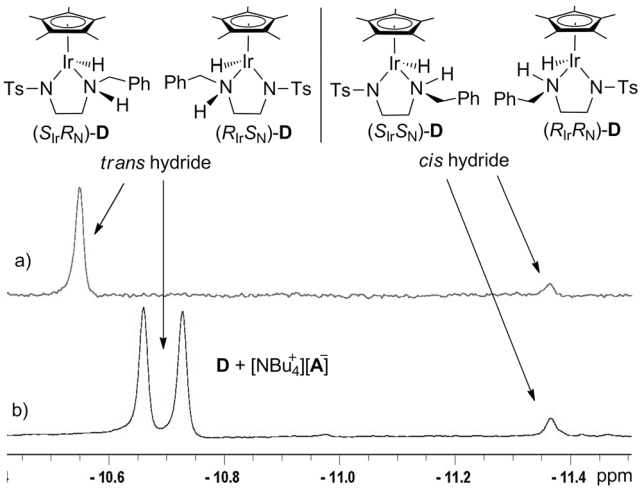

Figure 1. ^{1}H NMR spectra in [D$_8$]toluene (0.5 mL) at 20 °C of a) **D** (0.05 mmol) and b) **D** + [NBu$_4^+$][**A**$^-$] (0.1 mmol).

Racemic **D** can be generated as a solid precipitate in toluene by hydrogenation of the neutral **C** (Scheme 2). The *trans* hydride ($S_{Ir}R_N$)-**D** and its mirror image, in which the Ir-H and N-H hydrogens are *trans* disposed, have been characterized by X-ray crystallography (Scheme 2; Appendix I in the Supporting Information). The ^{1}H NMR spectrum of **D** displays two hydride resonances (δ_H, 20 °C in CD_2Cl_2: *trans*-**D** = −10.81, *cis*-**D** = −11.74; in [D$_8$]toluene: *trans*-**D** = −10.55, *cis*-**D** = −11.37 ppm) in the ratio of 10.5:1.

By using ^{1}H 2D-NOESY NMR measurements taken under 20 bar H_2, we are able to assign these signals to *trans*-($S_{Ir}R_N$)-**D** and its mirror image, and to the analogous *cis*-($S_{Ir}S_N$)-**D** and its enantiomer (Figures S1 and S2 in the Supporting Information), *trans*-**D** being the more abundant. Remarkably, the enantiomers of *trans*-**D** can be resolved in a [D$_8$]toluene solution by addition of [NBu$_4^+$][**A**$^-$] (Figure 1). The enantiomers of the *cis* hydride could not be resolved, however. Further support for the presence of additional isomers of **D** in solution is found in the X-ray crystal structure of the analogous chloride complex **E** (Scheme 2; Appendix II in the Supporting Information), in which two *trans* and one *cis* isomers are seen.

Under catalytic conditions, the hydride **D**, produced from hydrogenation of [**C**$^+$][**A**$^-$], is also racemic and can be precipitated and isolated by performing the hydrogenation in the presence of 2,6-lutidine in toluene. When **D** was used in the stoichiometric reduction of [**1a**$^+$][**A**$^-$] at 20 °C in toluene (Section 7 in the Supporting Information), **2a** was formed with the same *ee* (95%) as obtained under catalytic conditions, thus suggesting that the asymmetric induction of the catalysis arises in the hydride transfer step, rather than from enantioselective generation of **D**. However, under the same conditions, the neutral imine **1a** cannot be reduced. This observation, which resembles those made in related studies,[5] indicates that it is the iminium cation that participates in the hydride transfer.

Monitoring the ^{1}H NMR spectra of stoichiometric reactions of racemic **D** with imine and **HA** in the hydride region reveals trimolecular interactions. Thus, addition of **1a** to a solution of **D** at −50 °C does not appear to affect the hydrides (Figure 2a,b), consistent with **1a** not being reduced by **D**. However, on addition of one equivalent of **HA** at −50 °C, [**1a**$^+$][**A**$^-$] is formed instantly, and new resonances are seen in both the hydride region, $\delta_H = -9.25$ and −9.45 ppm (Figure 2c), and at low field in the region expected for hydrogen-bonded N-H in **D**, $\delta_H = 10.00$ and 10.34 ppm with an intensity ratio similar to that of the two new hydride peaks.

To gain insight into the hydrogen bonding between [**A**$^-$], the iminium cation, and the Ir-hydride, we treated the chloride complex **E** with 20 bar H_2 in CD_2Cl_2 in the presence of NaBARF (sodium tetrakis[3,5-bis(trifluoromethyl)phe-

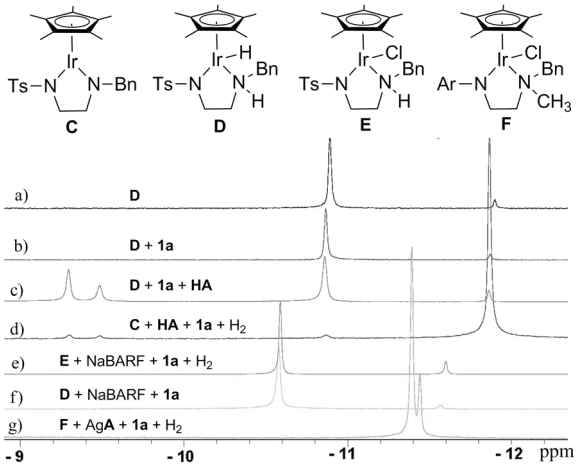

Figure 2. ^{1}H NMR spectra (0.5 mL CD_2Cl_2) of a) hydride **D** (0.05 mmol; −50 °C); b) (a) + **1a** (10 equiv); c) (b) + **HA** (1 equiv); d) **C** (0.1 mmol) + **HA** (1 equiv), followed by **1a** (10 equiv) and 20 bar H_2 at −78 °C; spectrum recorded at −50 °C; e) **E** (0.05 mmol) + NaBARF (2 equiv) + **1a** (10 equiv); 20 bar H_2 charged at −78 °C and spectrum recorded at −50 °C; f) **D** + NaBARF (2 equiv) + **1a** (10 equiv); g) **F** (0.1 mmol, Ar = 2,4,6-triisopropylphenylsulfonyl) + silver phosphate (1 equiv) + **1a** (10 equiv); 20 bar H_2 charged at −78 °C and spectrum recorded at −50 °C.

nyl]borate) and excess **1a**; this afforded only the racemic hydride **D** with no hydrogen-bonded hydrides observed (Figure 2e,f).[8] Unlike the phosphate [$\mathbf{A}^-$], the $BARF^-$ anion is not expected to act as a hydrogen-bond acceptor. Similarly, on hydrogenation of [$\mathbf{F}^+$][$\mathbf{A}^-$] (Figure 2g), in which the NH hydrogen atom is replaced with a methyl group, only two hydrides, at −11.39 and −11.44 ppm, were observed in the ^{1}H NMR spectrum, with no observable hydrogen-bonded species. Furthermore, when **D** was mixed with [NBu_4^+][$\mathbf{A}^-$], no new hydride resonances were observed in CD_2Cl_2, in contrast to the case of **D** being mixed with [$\mathbf{1a}^+$][$\mathbf{A}^-$]. These observations suggest that in the hydrogen-bonded network formed by **D**, [$\mathbf{1a}^+$], and [$\mathbf{A}^-$], the NH hydrogen atoms of the former two form hydrogen bonds with the oxygen atom of the latter. The importance of hydrogen bonding was further elucidated by catalytic reactions (Sections 7 and 8 in the Supporting Information), which indicate that it is the intermolecular hydrogen bonding that makes enantioselective hydrogenation of **1a** possible, at the expense of reaction rate, however, owing to the bulkiness of the bonded species.

We also monitored, by in situ ^{1}H NMR spectroscopy, the reaction of [$\mathbf{C}^+$][$\mathbf{A}^-$] under 20 bar H_2 in the presence of excess of **1a** when the temperature was raised from −78 to 20 °C. At low temperature (−50 °C), both **D** (*trans* and *cis* isomers) and the hydrogen-bonded hydrides were observed (Figure 2d). At this temperature no observable hydrogenation took place. However, contrary to the reaction at higher temperature, the *cis* hydride is favored. On raising the temperature, the *trans* isomer becomes the major species observed, and subsequent cooling does not alter the equilibrium, consistent with a kinetic effect. The lower activation energy characterizing formation of the *cis* hydride may be a result of hydrogen-bonding-assisted heterolysis of H_2 (Figure S3 in the Supporting Information).[9] Comparing the spectra (d) and (c) in Figure 2 shows that the intensity of the hydrogen-bonded hydrides varies with that of free *trans*-**D**, thus suggesting that the hydrogen-bonded hydrides arise from the *trans* hydrides.

Further ^{1}H NMR monitoring using an internal standard suggests that it is the minor *cis* hydride that hydrogenates [$\mathbf{1a}^+$] (Figure 3). We started from the free racemic hydride **D** with a ratio of free *trans* to free *cis* hydride 10.8:1 at −50 °C in the presence of ten equivalents of **1a** (Figure 3a). After addition of one equivalent of **HA** at the same temperature, two peaks can be seen between −9.2 and −9.6 ppm. The ratio of these two peaks added together to the free *trans* and *cis* hydride is approximately 7:7:1, indicating again that the new hydrogen-bonding hydrides derive from *trans*-**D** (Figure 3b). Increase of the temperature led to continued decrease in the content of the *cis* hydride, and this is accompanied with the appearance of amine product at −20 °C. Thus, comparing the conditions (a) and (g), the ratio of free *trans* to free *cis* hydride has changed from approximately 10.8:1 to 20:1. These observations suggest, surprisingly, that the minor *cis* hydride hydrogenates [$\mathbf{1a}^+$], instead of the major *trans* hydride, which forms observable hydrogen bonds with the organocatalyst; this inference is reminiscent of the observations made in the seminal study of asymmetric hydrogenation of dehydroamino acids with Rh–diphosphine catalysts.[10]

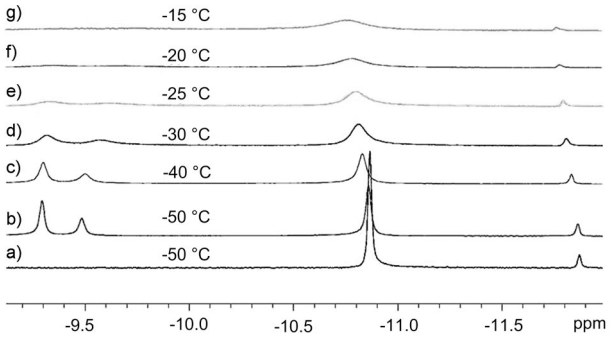

Figure 3. ^{1}H NMR monitoring of hydride transfer from **D** to **1a** in CD_2Cl_2 at various temperatures. Conditions: a) **D** (0.05 mmol) + **1a** (10 equiv); b–g) (a) + **HA** (1 equiv).

Taken together, the results above suggest that the enantioselective hydrogenation is likely to proceed via a hydrogen-bonded supramolecular complex[11] involving all three of **D**, [$\mathbf{1a}^+$], and [$\mathbf{A}^-$]. To shed light on the structure of the ternary complex, we have performed ^{1}H PFGSE, ^{1}H-^{13}C HSQC, ^{1}H NOESY NMR and DFT/PM6 computational studies of the model complex **E**, **HA**, and **1a** or **1h**.[12–13] Pulsed field-gradient spin echo (PFGSE) measurements were used to probe interactions between the components, while the identification of NOE signals allowed the nature of the interactions to be revealed and set constraints for subsequent computational modeling.

^{1}H DOSY NMR spectra of [$\mathbf{1h}^+$][$\mathbf{A}^-$], of a mixture of **HA** and **E**, and of a mixture of **E**, **HA**, and **1h** in the same concentration (0.1 mmol in 0.5 mL CD_2Cl_2) indicate that in the first two cases the components diffuse together, while in the last case part of the three species diffuse together.[14] Calculation of the hydrodynamic radii of each case shows that there is good agreement between the experimental hydrodynamic radii obtained from the NMR measurements and DFT/PM6 calculations (Section 15 in the Supporting Information). For example, the experimental hydrodynamic radius of the diffusing species in the mixture of **E**, **HA**, and **1h**, r_H = 7.89 Å, is in close agreement with the computed radius of the supramolecular complex incorporating **E** hydrogen-bonding to [$\mathbf{1h}^+$][$\mathbf{A}^-$], r_H = 7.20 Å.

Further, the ^{1}H-^{13}C HSQC and ^{1}H NOESY NMR spectra of a mixture of **HA** (0.1 mmol), **E** (1 equiv), and **1a** (1 equiv) at 800 MHz in CD_2Cl_2 (0.5 mL) allowed the identification of a range of NOE signals. Among these, two NOE signals were identified as being unambiguously derived from the ternary complex. They arise from the methoxy group of [$\mathbf{1a}^+$] and the isopropyl-substituted aryl ring of [$\mathbf{A}^-$], and the methyl group of [$\mathbf{1a}^+$] and the tosyl ring of **E** (Section 13 in the Supporting Information), thus supporting the hypothesized supramolecular complex.

These NOE signals were then taken as constraints in structural calculation and optimization. A range of structures were generated by conformational searching using molecular mechanics; the most popular structures, which satisfied the key NOE signals, were optimised using the DFT (B3LYP functional) followed by the PM6 method owing to the complexity of the system (Section 13 in the Supporting

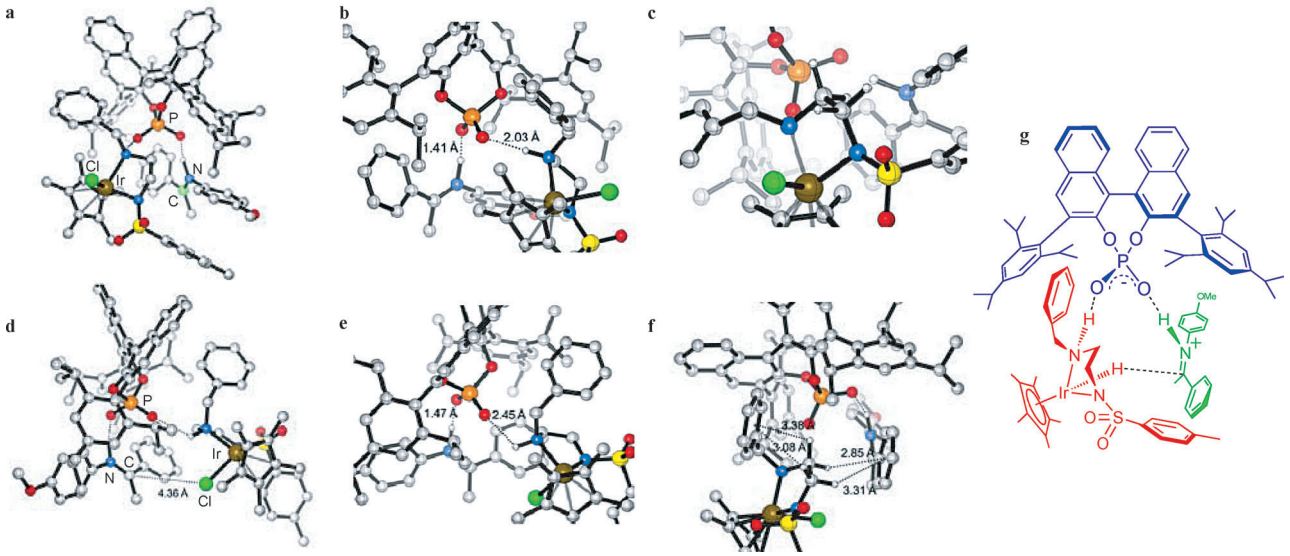

Figure 4. Modeled structures of ternary complexes. a, b) [($R_{Ir}S_N$)-**E**][**1a**$^+$][**A**$^-$] (−2.7 kcal mol^{-1}), arising from *trans*-($R_{Ir}S_N$)-**E**, [**1a**$^+$], and [**A**$^-$]; the structure fits NOE results; c) expansion of [($R_{Ir}S_N$)-**E**][**1a**$^+$][**A**$^-$] showing lack of CH–π interactions; d, e) [($S_{Ir}S_N$)-**E**][**1a**$^+$][**A**$^-$] (−5.7 kcal mol^{-1}), arising from *cis*-($S_{Ir}S_N$)-**E**, [**1a**$^+$], and [**A**$^-$]; the structure fits NOE results; f) expansion of [*cis*-($S_{Ir}S_N$)-**E**][**1a**$^+$][**A**$^-$] to show CH–π interactions; g) representation of the presumed transition state of hydride transfer in hydrogenation with the achiral and chiral catalysts **C** and **HA**. in (a–f): N blue, Cl green, Ir gold, O red, P orange, S yellow.

Information).[15] This led to two ternary structures consistent with the NOE data (Figure 4), the complex [($R_{Ir}S_N$)-**E**][**1a**$^+$][**A**$^-$] (−2.7 kcal mol^{-1}) incorporating *trans*-($R_{Ir}S_N$)-**E** (Figure 4a, b), and a lower-energy *cis* analogue [($S_{Ir}S_N$)-**E**][**1a**$^+$][**A**$^-$] (−5.7 kcal mol^{-1}; Figure 4d, e). In both structures, a hydrogen bond exists between the NH proton of [**1a**$^+$] and an oxygen atom of the phosphate, the O···H distances being similar at 1.41 Å and 1.47 Å, respectively. The other phosphate oxygen forms a hydrogen bond with the NH proton of **E**; however, the O···H distance is significantly shorter in the *trans* complex, 2.03 Å vs. 2.45 Å, indicating a weaker hydrogen bond in the *cis* analogue and thus explaining why hydrogen bonding with the *cis* hydride **D** was not observed.

Significantly, in the *trans*-**E**-derived complex [($R_{Ir}S_N$)-**E**][**1a**$^+$][**A**$^-$], the chloride faces away from the hydrogen-bonded [**1a**$^+$] (Figure 4a, b), whereas in the *cis* analogue the chlorine atom faces the *re*-face of [**1a**$^+$] with a Cl and C (C=N) separation of 4.36 Å (Figure 4d, e). The cis analogue would afford the observed *S*-configured amine, if the chloride of **E** was replaced with a hydride, thereby lending support to the NMR study above using the hydride **D**.

In addition to the hydrogen bonding, a range of CH–π interactions are evident in both complexes.[16] The main difference between the two ternary complexes is seen in the *cis*-**E**-derived [($S_{Ir}S_N$)-**E**][**1a**$^+$][**A**$^-$], which exhibits favorable CH–π interactions, ranging from 2.8 to 3.2 Å, between the CH_2 groups on the backbone of **E** and the benzyl phenyl ring of **E**, and between the former and the phenyl group of [**1a**$^+$] (Figure 4f). These interactions are absent in the *trans* analogue, thus accounting for the higher stability of the complex derived from *cis*-($S_{Ir}S_N$)-**E** (Figure 4c vs. f).

The results obtained with the model chloride complex **E** support the notion that a ternary complex is formed in the catalysis and is responsible for enantioselective hydride transfer, and further suggest that of the four isomeric hydrides **D**, the minor *cis*-($S_{Ir}S_N$)-**D** isomer forms the productive ternary complex with the phosphate and an iminium ion, through which the imino bond is reduced. The phosphate binds to both *cis*-($S_{Ir}S_N$)-**D** and [**1a**$^+$] through hydrogen-bonding and CH–π interactions, allowing the hydride to add only to the *re*-face of the imino bond. These interactions and the resulting ternary complex are proposed to be the key feature of the transition state of hydride transfer in the catalysis (Figure 4g), which permits highly effective chirality transfer, but a much slower rate of hydride transfer than in hydrogenation using non-hydrogen-bonding counteranions (Sections 7 and 8 in the Supporting Information).

In summary, this study has revealed that when an organometallic catalyst is combined with an organocatalyst to effect a reaction, nonconvalent interactions likely dictate the catalytic activity and selectivity, resembling enzymatic catalysis. The insight gained is anticipated to be of value for the design of future metal–organo cooperative catalysts.

Received: November 1, 2012
Published online: January 7, 2013

Keywords: Brønsted acid · cooperative catalysis · hydrogenation · iridium · noncovalent interactions

[1] a) *Organocatalysis* (Eds.: M. T. Reetz., B. List, S. Jaroch, H. Weinmann), Springer, Berlin, **2008**; b) R. R. Knowles, E. N. Jacobsen, *Proc. Natl. Acad. Sci. USA* **2010**, *107*, 20678–20685.
[2] For examples, see: a) M. Yamakawa, I. Yamada, R. Noyori, *Angew. Chem.* **2001**, *113*, 2900–2903; *Angew. Chem. Int. Ed.* **2001**, *40*, 2818–2821; b) Z. Y. Ding, F. Chen, J. Qin, Y. M. He,

Q. H. Fan, *Angew. Chem.* **2012**, *124*, 5804 – 5808; *Angew. Chem. Int. Ed.* **2012**, *51*, 5706 – 5710.

[3] Reviews: a) Z. H. Shao, H. B. Zhang, *Chem. Soc. Rev.* **2009**, *38*, 2745 – 2755; b) C. Zhong, X. Shi, *Eur. J. Org. Chem.* **2010**, 2999 – 3025; c) M. Rueping, R. M. Koenigs, J. Atodiresei, *Chem. Eur. J.* **2010**, *16*, 9350 – 9365; d) A. E. Allen, D. W. C. MacMillan, *Chem. Sci.* **2012**, *3*, 633 – 658; e) L. Stegbauer, F. Sladojevich, D. J. Dixon, *Chem. Sci.* **2012**, *3*, 942 – 958; f) Z. K. Yu, W. W. Jin, Q. B. Jiang, *Angew. Chem.* **2012**, *124*, 6164 – 6177; *Angew. Chem. Int. Ed.* **2012**, *51*, 6060 – 6072; g) Z. Du, Z. Shao, *Chem. Soc. Rev.* **2013**, DOI: 10.1039/C2CS35258C.

[4] a) "Highly Enantioselective Synthesis of Amines by Asymmetric Hydrogenation": C. Q. Li, PhD Thesis, University of Liverpool **2009**; b) W. J. Tang, S. Johnston, J. Iggo, J. L. Xiao, unpublished. For related studies, see: c) M. Rueping, R. M. Koenigs, *Chem. Commun.* **2011**, *47*, 304 – 306; d) S. L. Zhou, S. Fleischer, K. Junge, M. Beller, *Angew. Chem.* **2011**, *123*, 5226 – 5230; *Angew. Chem. Int. Ed.* **2011**, *50*, 5120 – 5124.

[5] C. Wang, B. Villa-Marcos, J. L. Xiao, *Chem. Commun.* **2011**, *47*, 9773 – 9785, and references therein.

[6] a) A. Macchioni, *Chem. Rev.* **2005**, *105*, 2039 – 2073; b) J. Lacour, D. Moraleda, *Chem. Commun.* **2009**, 7073 – 7089; c) R. J. Phipps, G. L. Hamilton, F. D. Toste, *Nat. Chem.* **2012**, *4*, 603 – 614.

[7] An in-depth study of similar salts: M. Fleischmann, D. Drettwan, E. Sugiono, M. Rueping, R. M. Gschwind, *Angew. Chem.* **2011**, *123*, 6488 – 6493; *Angew. Chem. Int. Ed.* **2011**, *50*, 6364 – 6369.

[8] [Na][BARF] affects the chemical shifts of **D**: compare the spectra (a) and (b) with (f) in Figure 2.

[9] M. Lei, W. Zhang, Y. Chen, Y. Tang, *Organometallics* **2010**, *29*, 543 – 548.

[10] a) J. Halpern, *Science* **1982**, *217*, 401 – 407; b) J. M. Brown, P. A. Chaloner, *J. Am. Chem. Soc.* **1980**, *102*, 3040 – 3048.

[11] a) D. Uraguchi, Y. Ueki, T. Ooi, *Science* **2009**, *326*, 120 – 123; b) P. Dydio, C. Rubay, T. Gadzikwa, M. Lutz, J. N. H. Reek, *J. Am. Chem. Soc.* **2011**, *133*, 17176 – 17179.

[12] **1h** is (*E*)-4-methoxy-*N*-(1-(4-nitrophenyl)ethylidene)aniline, which is more stable than **1a** and hence was used for experiments requiring relatively long time.

[13] The hydride **D** could not be used owing to its reaction with [**1a**$^+$] or [**1h**$^+$] under the conditions used.

[14] The X-ray structure of **1h** with **HA**: R. I. Storer, D. E. Carrera, Y. Ni, D. W. C. MacMillan, *J. Am. Chem. Soc.* **2006**, *128*, 84 – 86.

[15] Use of PM6 program: M. Ciardi, F. Tancini, G. Gil-Ramírez, E. C. Escudero Adán, C. Massera, E. Dalcanale, P. Ballester, *J. Am. Chem. Soc.* **2012**, *134*, 13121 – 13132.

[16] A review of CH – π interactions: M. Nishio, *Tetrahedron* **2005**, *61*, 6923 – 6950.

[17] CCDC-888491 and 888492 contain the supplementary crystallographic data for this paper. These data can be obtained free of charge from The Cambridge Crystallographic Data Centre via www.ccdc.cam.ac.uk/data_request/cif.

